

Received 8 June 2022, accepted 24 June 2022, date of publication 1 July 2022, date of current version 11 July 2022.

Digital Object Identifier 10.1109/ACCESS.2022.3187743

RESEARCH ARTICLE

Bipartite Tracking Formation Control of Nonlinear Multi-Agent Systems Using Adaptive Output–Feedback Protocols

LU LIU, DAN LIU¹, YUHANG MA¹, CHENYU YANG, HUIYU ZHANG, BIN YAO, ZENGXING ZHANG, ZHIDONG ZHANG, AND CHENYANG XUE¹

State Key Laboratory of Dynamic Measurement Technology, North University of China, Taiyuan 030051, China

Corresponding authors: Dan Liu (liudan235@nuc.edu.cn) and Zhidong Zhang (zdzhang@nuc.edu.cn)

This work was supported in part by the National Natural Science Foundation of China under Grant 62001428, in part by the Key Research and Development Program of Shanxi Province under Grant 202102020101010, in part by the National Natural Science Foundation of China as National Major Scientific Instruments Development Project under Grant 61727806, in part by the Shanxi “1331 Project” Key Subject Construction under Grant 1331KSC, and in part by the Scientific and Technological Innovation Programs of Higher Education Institutions in Shanxi under Grant 2020L0309.

ABSTRACT This paper proposed distributed adaptive formation control for leader-follower bipartite time-varying formation (BTVF) of a nonlinear multi-agent system (MAS). The proposed nonlinear MAS satisfies the one-sided Lipschitz-type condition. In the topological graphs with directed spanning trees, the design of adaptive protocols does not depend on the known communication topology, which can avoid the use of global information. Given limited information, the proposed MAS can achieve desired formation tracking by utilizing an observer protocol and converting the bipartite formation control problem into a stability problem of system errors. The analysis results of the systematic errors by using Lyapunov candidate functions, indicate that the MAS can be globally stable with a certain convergence rate during operation. Finally, numerical simulations are presented to confirm the validity of the proposed approach.

INDEX TERMS Bipartite time-varying formation, leader-follower system, nonlinear dynamics, adaptive control, competition network.

I. INTRODUCTION

There has been the development and progress of high technology and modern science in recent years, multi-agent systems (MASs) [1], [2] emerge and are gradually applied as a modern form of local warfare or the resource exploration process. An agent, is a powered system that is applied to aircraft, satellites, mobile robots, autonomous underwater vehicles (AUVs), and unmanned aerial vehicles (UAVs) with a microprocessor [3]–[7]. Compared with a single multifunctional agent, the cooperative control of MASs is characterized by autonomy, distribution, coordination and independent learning ability, with strong robustness to external influences and high tolerance to the failure of a single agent. Especially, many cooperative control tasks of MASs focus on

consensuses control, such as swarming, flocking, task assignment, formation control, and distributed estimation [8]–[14]. Vicsek [15] studied the consensus problem of particle swarms, which provided the basis for later work on the consensus problem. Jadbabaie *et al.* [16] analyzed and explained the convergence phenomenon of the simplified model proposed by Vicsek. They neglected the effect of disturbing inputs and introduced algebraic graph theory as an analysis tool. Olfati-Saber *et al.* [12] studied the basic conditions for MASs to achieve consensus in the case of fixed and switched topologies. Also, they separately analyzed the effect of the presence of time delay on the convergence of MAS in different topologies. Dong [17] designed a formation control protocol for UAVs with switching topologies and studied the necessary conditions for time-varying formation. Guo [18] proposed a control strategy that uses only the relative position information of neighboring agents to form a formation of

The associate editor coordinating the review of this manuscript and approving it for publication was Jinquan Xu¹.

multiple autonomous robots around a moving target. The controller was designed by combining target tracking and cooperative control of each robot. A distributed adaptive control strategy with real-time update was designed [19] for linear MASs to reduce the calculation, and the introduced adaptive parameters improved the self-adjustment ability of the event-triggering mechanism. A control algorithm based on neural networks was proposed [20] to achieve consensus of MAS, which consumes less energy. Distributed control of nonlinear MASs using multiple tools in [21]–[23]. Neural networks with high complexity cause limited computational real time. Low-complexity control systems without neural networks, adaptive control, and estimators have limited ability to self-regulate and control decisions based on real-time changes in the MAS formation state. The simplicity and inherent nonlinearity of the Lagrangian system model make this approach inappropriate for time-varying formation control in practical situations with uncertain, incomplete constraints.

Most of the previous studies tend to focus on the cooperative behavior of agents within a cluster. However, in practical scenarios, with increasing system scale and complexity, the MASs can be clustered to achieve attack, obstacle avoidance, or defense. Therefore, to enrich the diversity of tasks, the agents are always divided into competing subsystems. It can be observed in many scenarios in life (e.g., employees work as a team to improve the company's performance, but they also compete with each other in private groups). Inspired by the cooperative control of MAS, Altafini [24] proposed a control method with competing relationships based on Laplacian linear and nonlinear feedback. For achieving the consensus of distributed bipartite tracking, an adaptive fully distributed control protocol was proposed for linear MASs in [25]. This protocol is suitable for the case where the follower cannot receive the leader's information and the leader's control input is nonzero. The above-mentioned control methods have a common point in solving the global feedback by the Laplacian matrix. However, this reduces the operational efficiency of the system greatly, and the methods are not applicable under the failure of an individual or a variable system membership. To reduce the burden of communication networks and increase the flexibility of MASs, this paper adopts a control protocol that does not rely on Laplacian eigenvalues and can complete time-varying formation tracking using only the output information of neighboring agents when the formation joins or splits agents. In [26], an adaptive non-smooth protocol was proposed based on output information to achieve BTVF control of MASs. These studies provide a reference for the research of nonlinear MASs.

In the above study of MASs, the dynamics of individual agents were set to be linear to simplify the research, but many systems are nonlinear in practice. For AUVs [27], [28], it can not be neglected that the main source of external disturbance in operation is composed of underwater turbulence and waves. The control protocol that can resist external disturbances effectively is the fundamental guarantee for the AUV to accomplish its mission. Therefore, the formation control

problem of nonlinear systems is significant in practical applications [3], [29]. It should be noted that most of the studies on MASs require pre-determined information. Nevertheless, in practical applications, the information of the system is difficult to obtain accurately. Adaptive control combines parameter estimators, which can generate parameter estimates and combine them with control laws in real-time to control various types of systems with unknown or time-varying parameters. The bipartite formation control problem with mixed impulses for nonlinear MASs under an undirected graph was solved in [30]. In [31], an adaptive control method based on a finite-time scheme was proposed for solving the bipartite consensus where the state of each agent was unknown and the MAS system was nonlinear. Researchers combined adaptive control strategies with impulse control techniques to better solve the cooperative control of MASs [32], [33]. For achieving an adaptive bipartite tracking in the nonlinear MASs, Yu and Lin [34] proposed a filtering backstepping algorithm based on distributed fuzzy command, and an error compensation vector was constructed to compensate for the errors generated by the filter to solve the adaptive bipartite tracking problem of nonlinear MAS. A distributed control protocol based on neighbor state was proposed in [35] to achieve bipartite consensus of MAS when the leader input is unknown. Currently, there are more relevant studies based on state feedback and few cases of using distributed adaptive control protocols based on output feedback to study the MASs with external disturbances of BTVF control.

The state information of each agent is inaccurate or unavailable in many cases. In order to realize the bipartite formation control of MASs with external disturbances, an adaptive control strategy based on output feedback is proposed. The main contributions of this paper are listed as follows: (i) The bipartite time-varying stratum problem for MASs with external disturbances is solved under the one-sided Lipschitz nonlinearity condition, which is more suitable for stratigraphic control in practical applications than the method of estimating nonlinear dynamics with neural networks. A distributed adaptive control protocol based on the local output information of neighboring agents as feedback is used, which is independent of the Laplacian matrix eigenvalue information. When the formation is reconstructed, the stability of the system is unaffected. (ii) The leader-follower bipartite time-varying formation tracking problem is investigated in the presence and absence of disturbances, respectively, when the control input of the leader is nonzero bounded and the state information of the leader is not globally known. In the numerical simulation section, the AUV noncomplete dynamics model is transformed into a complete dynamics model for computation and bounded random vectors are introduced to simulate external perturbations in this model, which is more suitable for formation control of aerospace systems, multi-UAV systems, and multi-AUV systems etc. in practical applications.

This paper contains five subsections. In **Section II**, the research background and research status of cooperative

control of MASs are introduced. In **Section III**, some mathematical fundamentals, lemmas, and knowledge about graph theory are presented. In **Section IV**, we give a model of a first-order nonlinear MAS, analyze the bipartite formation tracking problem, and design a control protocol based on dynamical output feedback. Constructing an error-based Lyapunov candidate function verified the stability of the system. **Section V** constructs and simplifies the model of AUV formation motion with fixed depth, and analyzes the effect of external disturbance on the formation motion through numerical simulation. The research content and results of this paper are presented in **Section VI**.

II. BACKGROUND AND PROBLEM STATEMENT

The definitions of mathematical symbols used in this article and some basic theorems are given, and also the basic definition and properties of weighted directed graphs are introduced.

A. PRELIMINARIES

- The real matrix and complex matrix with a size of $m \times m$ are represented as $\mathbb{R}^{m \times m}$ and $\mathbb{C}^{m \times m}$, respectively.
- The all zeros matrix and identity matrix with a size of $m \times n$ can be denoted as $O_{m \times n}$ and $I_{m \times n}$, respectively.
- For an arbitrary matrix $E \in \mathbb{R}^{n \times n}$, the minimum eigenvalue and maximum eigenvalue of E can be expressed as $\lambda_{\min}(E)$ and $\lambda_{\max}(E)$, respectively.
- In A^T , the symbol T indicates the transpose of matrix A .
- The H positive definite (positive semidefinite) can be represented by $H > 0$ ($H \geq 0$).
- $U \otimes V$ represents the Kronecker product of U and V . The further operation rules for the two matrices are as follows:
 - (1) $U \otimes (V + W) = U \otimes V + U \otimes W$,
 - (2) $(U \otimes V)(W \otimes X) = (UW) \otimes (VX)$.
- The signum function $\text{sgn}(\cdot)$ was defined as

$$\text{sgn}(i) = \begin{cases} 1, & i > 0 \\ 0, & i = 0 \\ -1, & i < 0 \end{cases}$$

B. BASIC ALGEBRAIC GRAPH THEORY

Agents transmit information to achieve cooperative control by communicating with other agents in the group. Establishing the communication topology between agents with directed graphs is a more common approach to the modeling process. In a weighted digraph [26] $\mathcal{G} = \{\vartheta, \mathcal{E}, \mathcal{A}\}$, the nonempty finite set of nodes is represented as $\vartheta = \{v_1, \dots, v_N\}$. $\mathcal{E} \subseteq \vartheta \times \vartheta$ is a set of communication edges or arcs between N agents. Setting the weights of the edges a_{ij} , the digraph can be expressed by the adjacency matrix $\mathcal{A} = [a_{ij}]$. Two nodes are called adjacent if there is an edge between them. It is worth noting that for digraph \mathcal{G} , a line from node i to node j can be denoted as $v_{ij} = (v_i, v_j)$. A directed graph is called bidirectional if the edge between individual nodes are bidirectional, i.e., any two points can communicate in both

directions. In the weighted adjacency matrix \mathcal{A} , the signed weight a_{ij} ($a_{ij} \neq 0$) can be negative or positive. Specifically, if $a_{ij} > 0$, the i_{th} agent and the j_{th} agent are mutually cooperative, conversely, they are competitive. However, a_{ij} can only be non-negative in an undirected graph. Therefore, the consensus control of digraph is more appropriate and challenging than of undirected graphs.

Furthermore, if a path exists between node i and any other node, the digraph is strongly connected. The weighted Laplacian matrix $L = [l_{ij}]$ of the digraph \mathcal{G} be constructed as follows:

$$l_{ij} = \begin{cases} \sum_{j=1, j \neq i}^N |a_{ij}|, & i = j, \\ -a_{ij}, & i \neq j. \end{cases} \quad (1)$$

Since no follower can convey information to the leader, i.e., no arrow can point to the leader, the relevant weighted Laplacian matrix L as follows:

$$L = \begin{bmatrix} 0 & 0_{1 \times N} \\ L_2 & L_1 \end{bmatrix} \quad (2)$$

where $L_1 = \mathbb{R}^{N \times N}$, and $L_2 = -[a_{10}, a_{20}, \dots, a_{N0}]^T \in \mathbb{R}^{N \times 1}$.

Lemma 1 [36]: Each row of the weighted Laplacian matrix sums to zero and contains at least one eigenvalue of 0. Concerning matrix L , several statements are equivalent as follows:

- (1) \mathcal{G} is balanced structurally.
- (2) The gauge transformed \mathcal{A} is equal to a non-negative matrix.
- (3) $\lambda_{\min}(L) = 0$.

Definition 1 [24]: If the set represented by all agents is separated into two subsets V_a and V_b without intersection, the digraph \mathcal{G} is structurally balanced. Two subsets satisfy the following conditions:

- (1) $V_a \cup V_b = V$ and $V_a \cap V_b = \emptyset$.
- (2) $\begin{cases} a_{ij} \geq 0, & \forall i, j \in V_a, \\ a_{ij} \leq 0, & \forall i \in V_a, j \in V_b, \end{cases} \quad a \neq b (a, b = 1, 2)$.

For the convenience of distinguishing to which subset the agents belong and using the gauge transformations in [24], introduce a matrix $\mathcal{D} = \text{diag}(d_1, d_2, \dots, d_N)$, $D \in \mathcal{D}$. The value of d_i satisfies the following conditions:

$$\begin{cases} d_i = 1, & i \in V_a, \\ d_i = -1, & i \in V_b, \end{cases}$$

Lemma 2 [37]: For a digraph where all nodes can be divided into two subsets, there exists a transformation. The matrix D mentioned above satisfies that terms DAD have non-negative entries and DLD have all non-positive off-diagonal entries.

Lemma 3 [38] (*Schur Complement*): Supposing that the matrix $A = \begin{bmatrix} A_{11} & A_{12} \\ A_{12}^T & A_{22} \end{bmatrix}$ composed of A_{11} , A_{12} , and A_{22} are

symmetric matrices of appropriate dimensions, inequalities (1)-(3) are mutual equivalence:

$$\begin{aligned}
 (1) \quad & \begin{pmatrix} A_{11} & A_{12} \\ A_{12}^T & A_{22} \end{pmatrix} < 0, \\
 (2) \quad & A_{11} < 0 \quad \text{and} \quad A_{22} - A_{12}^T A_{11}^{-1} A_{12} < 0, \\
 (3) \quad & A_{22} < 0 \quad \text{and} \quad A_{11} - A_{12} A_{22}^{-1} A_{12}^T < 0. \quad (3)
 \end{aligned}$$

III. DEFINITION OF BIPARTITE FORMATION TRACKING

Measurement noise and unknown dynamical phenomena including friction, external disturbances are widely present in various industries such as aerospace, robotics, and automation and can affect their control performance. Therefore, disturbance suppression has been one of the fundamental issues in controller design. To address this issue, equations (4) and (5) are used to model the nonlinear dynamic system, and the corresponding control strategy is designed to maintain the multi-agent formation under external disturbance (e.g., formation maintenance when AUV formations are affected by ocean currents). Suppose that a nonlinear dynamic MAS is consisted of $N + 1$ agents in general time-varying states. The time-varying state vector (x_i) and output vector (y_i) are introduced to describe the dynamics equations of each agent. The dynamic equations for the N followers and leader are as follows:

Followers:

$$\begin{aligned}
 \dot{x}_i &= Ax_i + Bu_i + \Phi\omega(x_i), \\
 y_i &= Cx_i, \quad i = 1, 2, \dots, N. \quad (4)
 \end{aligned}$$

Leader:

$$\begin{aligned}
 \dot{x}_0 &= Ax_0 + Bu_0 + \Phi\omega(x_0), \\
 y_0 &= Cx_0, \quad (5)
 \end{aligned}$$

The connections between this system are represented by the digraph \mathcal{G} . The vector $x = [x_1^T, \dots, x_N^T]^T$ contains velocity and position information which is the global state vector. $x_0 \in \mathbb{R}^n$ is the leader's state; $u_i \in \mathbb{R}^p$ and $u_0 \in \mathbb{R}^p$ are the control input of the i_{th} agent and the leader; $\omega(x_i)$ and $\omega(x_0)$ denote the bounded exogenous disturbance of the i_{th} agent and the leader, respectively; $A \in \mathbb{R}^{m \times m}$ and $B \in \mathbb{R}^{m \times q}$, and $C \in \mathbb{R}^{p \times m}$ are constant matrices. The matrix $\bar{B} \in \mathbb{R}^{q \times m}$ is pseudo-inverse matrix satisfying $\bar{B}B = I_q$ ($B \in \mathbb{R}^{q \times m}$ is input matrix). The matrix $\tilde{B} \in \mathbb{R}^{(m-q) \times m}$ satisfying $\tilde{B}B = 0$ and $\begin{bmatrix} \bar{B}^T \\ \tilde{B}^T \end{bmatrix}^T$ is nonsingular.

Remark 1: In practical applications, with the change of time and missions, the topology relationship of each agent in the MAS varies subsequently. This paper only considers the fixed topology, and interested readers can refer to [39] for detailed information on topology variation.

Remark 2: There are two other types of control based on output feedback, "neural dynamics-based output feedback scheme" and "data-driven adaptive extended state observers for output feedback scheme." The neural dynamics-based output feedback approach used in literature [40] and [41]

can use neural networks to identify the system output quantities to obtain the unknown parameters of the controlled object. Compared with the traditional PID controller, the neural network has excellent approximation capability and strong robustness. However, as the complexity of the system increases, the number of neurons in the hidden layer of the neural network increases and the system runs slower. In addition, the neural network structure can only be selected empirically. Another output feedback method is the data-driven extended state observer (DAESO)-based adaptive control [42], [43], which can control the system using only input/output data and can simultaneously evaluate parameters such as input gain, total perturbation, and unknown velocity, and is suitable for dynamical models with unknown model parameters. The controller considers the effect of system input changes at the current moment and multiple past moments of system input changes on system output changes at the next moment, giving higher degrees of freedom and greater flexibility in controller design, but noise and disturbances in the system can seriously affect system stability due to the high dependence on input and output data.

Definition 2 [44]: Digraph \mathcal{G} is said to realize a bipartite formation tracking if x_i of i_{th} agent meets the conditions:

$$\begin{cases} \lim_{t \rightarrow \infty} \|x_i - f_i(t) - x_0\| = 0, & \forall i \in V_a \\ \lim_{t \rightarrow \infty} \|x_i - f_i(t) + x_0\| = 0, & \forall i \in V_b \end{cases} \quad (6)$$

where $f_i(t)$ is the bipartite formation control vector corresponding to i_{th} agent and $f = [f_1^T(t), \dots, f_N^T(t)]^T$. Based on **Definition 1**, equality (6) can be rewritten as:

$$\lim_{t \rightarrow \infty} \|x_i - f_i(t) - d_i x_0\| = 0, \quad i = 1, 2, \dots, N. \quad (7)$$

Before theoretical verification, we present some basic assumptions on system dynamics and connections between agents.

Assumption 1: The constant $u_{\max} > 0$, so that $\|u_0(t)\| < u_{\max}$.

Assumption 2 [11]: Suppose that the digraph \mathcal{G} is structurally balanced and the root node can reach any node along an edge, indicating there exists a directed spanning tree in the directed graph.

Assumption 3: The (A, B, C) is observable and controllable.

In **Assumption 1**, the boundedness of the control inputs ensures that all the agents eventually converge to a specific final value or a specific region. Controllability and observability represent the ability of the system input to effectively control the system state and the ability of the system output to respond exactly to the system state, respectively. Thus **Assumption 2** and **Assumption 3** are prerequisites for MAS to achieve consensus.

Define

$$\tilde{L} \triangleq DL_1D \quad (8)$$

Before proceeding to algorithm design and proof, two sufficient conditions for reaching consensus are given.

Lemma 4 [45]: If $\bar{L} \in \mathbb{R}^{m \times m}$ is nonsingular, there a matrix $R > 0$ make $R\bar{L} + \bar{L}^T R > 0$.

Lemma 5 [46] (*Barbalat's Lemma*): If the function $g(t)$ is derivable and has a finite limit as $t \rightarrow \infty$, if the first-order derivative $\dot{g}(t)$ is uniformly continuous, we have $\lim_{t \rightarrow \infty} \dot{g}(t) = 0$.

This paper aims to investigate the conditions satisfied by the control protocol when nonlinear MASs (4) and (5) can achieve bipartite formation.

Assumption 4: The nonlinear function $\omega(x_i)$ satisfies the Lipschitz condition as follows:

$$\|\omega(x_i) - \omega(x_j)\| \leq k \|x_i - x_j\|, \quad \forall x_i, x_j \in \mathbb{R}^n, \quad t > 0. \quad (9)$$

where $x_i, x_j \in \mathbb{R}^n$ and $k \in \mathbb{R}$ are constants. **Assumption 4** guarantees that there is an equilibrium point for the nonlinear MAS system and the solution of the model is available.

Assumption 5: Suppose the matrix $M \in \mathbb{R}^{p \times m}$ that satisfies $\Phi = BM$. This matrix can be combined with other terms to eliminate the nonlinear terms in the equation.

Theorem 1: Suppose matrix P satisfies **Assumptions 2-3** and the following inequality. The bipartite tracking formation of the nonlinear MASs can be solved by introduced the matrix P .

$$PA + A^T P - 2PBB^T P + k^2 PP + I_n < 0, \quad (10)$$

The information transmission between adjacent agents is realized accomplished through a communication topology network. For a system contains $N + 1$ agents, the state of leader serves as a reference state for the remaining N followers, and the follower remains at a specific distance and orientation from the neighbors to form the specified formation.

IV. DESIGN OF BIPARTITE FORMATION TRACKING CONTROL PROTOCOL

A control strategy is presented for solving the bipartite time-varying tracking formation of the MAS with external disturbance through output feedback. Where suppose each agent can obtain its own relative output information relative to its neighbors. In **Definition 1**, if $\lim_{t \rightarrow \infty} \|x_i - f_i(t) - d_i x_0\| = 0$, which means that the designed control strategy can solve the bipartite formation of MAS. The control input and the estimated state of i_{th} agent can be expressed as follows:

$$\begin{aligned} u_i &= cK(\hat{x}_i - \hat{\delta}_i) + v_i - d_i \theta_i (B^T P \tilde{x}_i) \\ \dot{\hat{x}}_i &= A\hat{x}_i + Bu_i + \Phi\omega(\hat{x}_i) + c_i FC(\hat{x}_i - x_i + f_i) \\ \dot{\hat{x}}_0 &= A\hat{x}_0 + Bu_0 + \Phi\omega(\hat{x}_0) + FC(\hat{x}_0 - x_0) \\ \dot{\hat{\delta}}_i &= A\hat{\delta}_i + FC\phi_i - d_i B\theta_i (B^T Q \bar{\phi}_i) \\ \dot{\hat{c}}_i &= \hat{x}_i^T PBB^T P \hat{x}_i \end{aligned} \quad (11)$$

Remark 3: For this system, two observers \hat{x}_i and $\hat{\delta}_i$ are created, and \hat{x}_i is the state value when the i_{th} agent form a desired formation obtained by calculation. Assuming that

only the output of each follower is known. Therefore it is necessary to design a state observer that helps to observe the unknown state of each agent, and \hat{x}_0 indicates the leader's observed state. $\hat{\delta}_i$ is each team reference state relative to the leader's state. The leader's team takes the leader as a reference, and the other team uses the opposite state of the leader as a virtual reference to maintain the desired formation. $\hat{\delta}_i$ is defined as follows:

$$\begin{cases} \hat{\delta}_i = \hat{x}_0, & d_i = 1 \\ \hat{\delta}_i = -\hat{x}_0, & d_i = -1 \end{cases}$$

where $c_i (c_i > 0)$ is the adaptive coupling weight of each i_{th} agent. Meanwhile, for the leader, $\hat{x}_0 = \delta_0$ and $\bar{\phi}_i = d_i \phi_i$, F and K are the control parameter and output feedback matrix, and they are determined later. v_i is the formation compositional vector, and it can be defined as $v_i = \bar{B}(\dot{f}_i - Af_i)$. Parameters ϕ_i and c are expressed as follows:

$$\begin{aligned} \phi_i &= \sum_{j=1}^N |a_{ij}| (\hat{\delta}_i - \text{sgn}(a_{ij}) \hat{\delta}_j) + a_{i0} (\hat{\delta}_i - d_i \delta_0) \\ c &= \text{diag}(c_1, \dots, c_N) \end{aligned} \quad (12)$$

Furthermore, $\theta_i(\cdot)$ is a nonlinear function that can be used for subsequent proofs. It is defined as follows:

$$\theta_i(\kappa) = \begin{cases} \frac{\kappa}{\|\kappa\|}, & \|\kappa\| \neq 0, \\ 0, & \|\kappa\| = 0, \end{cases} \quad \kappa \in \mathbb{R}^q \quad (13)$$

In this subsection, according to the formation control protocol (11) and **Assumption 5**, the dynamical equations of the nonlinear MASs in (4) and (5) can be transformed into:

$$\begin{aligned} \dot{x}_i &= Ax_i + cBK(\hat{x}_i - \hat{\delta}_i) + Bv_i \\ &\quad - d_i B\theta_i (B^T P \tilde{x}_i) + \Phi\omega(x_i), \\ \dot{\hat{x}}_i &= A\hat{x}_i + cBK(\hat{x}_i - \hat{\delta}_i) + Bv_i + \Phi\omega(\hat{x}_i) \\ &\quad - d_i B\theta_i (B^T P \tilde{x}_i) + c_i FC(\hat{x}_i - x_i + f_i), \\ \dot{\hat{x}}_0 &= A\hat{x}_0 + Bu_0 + \Phi\omega(\hat{x}_0) + FC(\hat{x}_0 - x_0). \end{aligned} \quad (14)$$

Proof: Let

$$\begin{aligned} \tilde{\varepsilon}_i &= x_i - f_i(t) - d_i x_0, \\ \tilde{x}_i &= \hat{x}_i - d_i \hat{x}_0, \end{aligned}$$

where $\tilde{\varepsilon}_i$ denotes the value of difference between the actual state and desired states for the desired formation; \tilde{x}_i indicates the formation error between the observed state of i_{th} agent and leader.

Simplifying equations (4), (5), and (14) yields

$$\begin{aligned} \dot{\tilde{\varepsilon}}_i &= A\tilde{\varepsilon}_i + cBK(\hat{x}_i - \hat{\delta}_i) + Bv_i + Af_i - \dot{f}_i \\ &\quad - d_i B(\theta_i(B^T P \tilde{x}_i) + u_0) + \Phi(\omega(x_i) - d_i \omega(x_0)). \end{aligned} \quad (15)$$

and

$$\begin{aligned} \dot{\tilde{x}}_i &= A\tilde{x}_i + cBK(\hat{x}_i - \hat{\delta}_i) - d_i B(\theta_i(B^T P \tilde{x}_i) + u_0) \\ &\quad \times c_i FC(\tilde{x}_i - \tilde{\varepsilon}_i) + \Phi(\omega(\hat{x}_i) - d_i \omega(\hat{x}_0)). \end{aligned} \quad (16)$$

Let

$$\begin{aligned} \tilde{\varepsilon} &= [\tilde{\varepsilon}_1^T, \tilde{\varepsilon}_2^T, \dots, \tilde{\varepsilon}_N^T]^T, \\ \tilde{x} &= [\tilde{x}_1^T, \tilde{x}_2^T, \dots, \tilde{x}_N^T]^T, \\ \tilde{\delta} &= [\tilde{\delta}_1^T, \tilde{\delta}_2^T, \dots, \tilde{\delta}_N^T]^T, \end{aligned}$$

According to (15) and (16), the global dynamic system can be simplified as:

$$\begin{aligned} \dot{\tilde{\varepsilon}} &= (I_N \otimes A) \tilde{\varepsilon} + (c \otimes BK)(\tilde{x} - \tilde{\delta}) + (I_N \otimes \Phi) \bar{W} \\ &\quad + (I_N \otimes B) v + (I_N \otimes A) f - (I_N \otimes I_n) \dot{f} \\ &\quad - (D \otimes B) \left(\theta \left(B^T P \tilde{x}_i \right) + I_N \otimes u_0(t) \right). \end{aligned} \quad (17)$$

$$\begin{aligned} \dot{\tilde{x}} &= [I_N \otimes (A + cBK)] \tilde{x} - (c \otimes BK) \tilde{\delta} + (I_N \otimes \Phi) \bar{W} \\ &\quad - (D \otimes B) \left(\theta \left(B^T P \tilde{x} \right) + I_N \otimes u_0(t) \right) \\ &\quad + (c \otimes FC)(\tilde{x} - \tilde{\varepsilon}). \end{aligned} \quad (18)$$

where $v = [v_1^T, v_2^T, \dots, v_N^T]^T$.

$$\bar{W} = \begin{bmatrix} \omega(\hat{x}_1) - d_1 \omega(\hat{x}_0) \\ \omega(\hat{x}_2) - d_2 \omega(\hat{x}_0) \\ \vdots \\ \omega(\hat{x}_N) - d_N \omega(\hat{x}_0) \end{bmatrix}. \quad (19)$$

Besides, according to the state information of the neighboring agents, let

$$r_i = \sum_{j=1}^N |a_{ij}| \left((x_i - f_i) - \text{sgn}(a_{ij}) (x_j - f_j) \right) + a_{i0} (x_i - f_i - d_i x_0) \quad (20)$$

Since $d_i x_0 = \text{sgn}(a_{ij}) d_j x_0$, equation (20) be simplified as:

$$r_i = \sum_{j=1}^N |a_{ij}| (\tilde{\varepsilon}_i - \text{sgn}(a_{ij}) \tilde{\varepsilon}_j) + a_{i0} \tilde{\varepsilon}_i \quad (21)$$

To facilitate stability analysis, the coordinate transformation is performed on equations (12), (18), and (21):

$$\begin{aligned} \bar{r} &= (L_1 \otimes I_n) \tilde{\varepsilon}, \\ \bar{x} &= (L_1 \otimes I_n) \tilde{x}, \\ \bar{\delta} &= (L_1 \otimes I_n) \tilde{\delta}, \end{aligned}$$

To simplify equations (20) and (21), let $\Omega = (I_N \otimes B) v + (I_N \otimes A) f - (I_N \otimes I_n) \dot{f}$ and $\Upsilon = \theta(B^T P \tilde{x}) + I_N \otimes u_0(t)$. We have:

$$\begin{aligned} \dot{\bar{r}} &= (I_N \otimes A) \bar{r} + (c \otimes BK)(\bar{x} - \bar{\delta}) \\ &\quad + (L_1 \otimes I_n) \Omega - (L_1 D \otimes B) \Upsilon + (L_1 \otimes \Phi) \bar{W}. \\ \dot{\bar{x}} &= [I_N \otimes (A + cBK)] \bar{x} - (L_1 D \otimes B) \Upsilon \\ &\quad - (c \otimes BK) \bar{\delta} + (c \otimes FC)(\bar{x} - \bar{r}) + (L_1 \otimes \Phi) \bar{W}. \end{aligned} \quad (22)$$

From **Assumptions 1-4**, the following equations hold:

$$\begin{aligned} \bar{B} A f_i - \bar{B} \dot{f}_i &= 0 \\ Q A - 2 C^T C + A^T Q &< 0 \\ A P^{-1} - 2 B B^T + P^{-1} A &< 0 \end{aligned} \quad (23)$$

There are appropriate scalars $\mu_1, \mu_2 > 0$, and the matrix $F = -Q^{-1} C^T$ is the solution of LMI (Linear matrix inequalities) (24), See Eq. 24, as shown at the bottom of the page.

To make the equations more convenient to calculate, let

$$\begin{aligned} \hat{r} &= (D \otimes I_n) \bar{r}, \\ \hat{x} &= (D \otimes I_n) \bar{x}, \\ \hat{\chi} &= \hat{x} - \hat{r}, \end{aligned} \quad (25)$$

According to **Assumption 3**, $\bar{L} = DL_1 D$ and $DD = I_N$. The derivatives of \hat{r} , \hat{x} and $\hat{\chi}$ in equation (25) are indicated as:

$$\begin{aligned} \dot{\hat{r}} &= (I_N \otimes A) \hat{r} + (c \otimes BK)(\hat{x} - \hat{\delta}) - (\bar{L} \otimes B) \Upsilon \\ &\quad + (DL_1 \otimes I_n) \Omega + (DL_1 \otimes \Phi) \bar{W}. \end{aligned} \quad (26)$$

$$\begin{aligned} \dot{\hat{x}} &= [(I_N \otimes (A + cBK))] \hat{x} - (c \otimes BK) \hat{\delta} - (\bar{L} \otimes B) \Upsilon \\ &\quad + (c \otimes FC) \hat{\chi} + (DL_1 \otimes \Phi) \bar{W}. \end{aligned} \quad (27)$$

$$\dot{\hat{\chi}} = (I_N \otimes (A + cFC)) \hat{\chi} - (DL_1 \otimes I_n) \Upsilon. \quad (28)$$

According to the definition of $B \in \mathbb{R}^{m \times q}$, $\bar{B} \in \mathbb{R}^{q \times m}$, $\tilde{B} \in \mathbb{R}^{(m-q) \times m}$ and condition (21), it is easy to obtain that $\tilde{B} B v_i + \bar{B} A f_i - \tilde{B} \dot{f}_i = 0$, and $\bar{B} B v_i + \bar{B} A f_i - \bar{B} \dot{f}_i = 0$. Then, $B v_i + A f_i - \dot{f}_i = 0$ can be obtained due to $\begin{bmatrix} \bar{B}^T \\ \tilde{B}^T \end{bmatrix}$ is a nonsingular matrix and $v_i = \bar{B}(\dot{f}_i - A f_i)$. Thus, \hat{r} is expressed as:

$$\dot{\hat{r}} = (I_N \otimes A) \hat{r} + (c \otimes BK)(\hat{x} - \hat{\delta} + (DL_1 \otimes \Phi) \bar{W}). \quad (29)$$

and the $\hat{\chi}$ is expressed as:

$$\dot{\hat{\chi}} = (I_N \otimes (A + cFC)) \hat{\chi}. \quad (30)$$

Let $e_i = \hat{x}_i - x_i$, $e_0 = \hat{x}_0 - x_0$ indicate the error between the actual state and the observed state of follower and leader.

According to equations (4), (5), and (10), we have:

$$\begin{aligned} e_i &= \hat{x}_i - \dot{x}_i \\ &= A e_i + \Phi(\omega(\hat{x}_i) - \omega(x_i)) + F C e_i, \end{aligned} \quad (31)$$

and

$$\begin{aligned} e_0 &= \hat{x}_0 - \dot{x}_0 \\ &= A e_0 + \Phi(\omega(\hat{x}_0) - \omega(x_0)) + F C e_0, \end{aligned} \quad (32)$$

$$\begin{bmatrix} Q A + A^T Q - 2 C^T C & * & * \\ * & Q A + A^T Q - 2 C^T C + 2 \mu_1 k I_N + 2 \mu_2 \rho I_N & Q B N - \mu_1 I_N + \mu_2 \eta I_N \\ * & * & -2 \mu_2 I_N \end{bmatrix} < 0 \quad (24)$$

Taking a Lyapunov candidate function for the observer errors consisting of (26)-(32), the result are presented as follows:

$$\begin{aligned}
 V_1 &= \sum_{i=1}^N \widehat{x}^T (I_N \otimes P) \widehat{x} + \sum_{j=1}^N (c_j - c_0)^2 \\
 &\quad + \sum_{i=1}^N \widehat{\chi}^T (I_N \otimes Q) \widehat{\chi}, \\
 V_2 &= \sum_{i=1}^N e_i^T Q e_i + e_0^T Q e_0, \tag{33}
 \end{aligned}$$

Based on the results from equations (26)-(30), the time derivative of V_1 being expressed as:

$$\begin{aligned}
 \dot{V}_1 &= \sum_{i=1}^N \widehat{x}^T (I_N \otimes P) \left([I_N \otimes (A + cBK)] \widehat{x} \right) \\
 &\quad - \sum_{i=1}^N \widehat{x}^T \left((c \otimes BK) \widehat{\delta} - (\bar{L} \otimes B) \Upsilon \right) \\
 &\quad + \sum_{i=1}^N \widehat{x}^T \left((c \otimes FC) (\widehat{x} - \widehat{r}) + (DL_1 \otimes \Phi) \bar{W} \right) \\
 &\quad + 2(c_i - c_0) \dot{c}_i + \sum_{i=1}^N \widehat{\chi}^T (I_N \otimes \Theta) \widehat{\chi}, \\
 &\leq \widehat{x}^T \left[I_N \otimes \left(PA + A^T P - 2c_0 PBB^T P \right) \right] \widehat{x} \\
 &\quad - 2 \widehat{x}^T (c \otimes PBK) \widehat{\delta} - 2 \widehat{x}^T (\bar{L} \otimes PB) \Upsilon \\
 &\quad + 2 \widehat{x}^T (c \otimes PFC) \widehat{\Theta} + 2 \widehat{x}^T (DL_1 \otimes P\Phi) \bar{W} \\
 &\quad + \sum_{i=1}^N \widehat{\chi}^T (I_N \otimes \Theta) \widehat{\chi}. \tag{34}
 \end{aligned}$$

When c_0 sufficiently large and $c_0 \geq 1$, we have:

$$\begin{aligned}
 \dot{V}_1 &\leq \widehat{x}^T \left[I_N \otimes \left(PA + A^T P - 2PBB^T P \right) \right] \widehat{x} \\
 &\quad + 2 \widehat{x}^T (DL_1 \otimes P\Phi) \bar{W} + \sum_{i=1}^N \widehat{\chi}^T (I_N \otimes \Theta) \widehat{\chi} \\
 &\quad - 2 \widehat{x}^T (c \otimes PBK) \widehat{\delta} - 2 \widehat{x}^T (\bar{L} \otimes PB) \Upsilon \\
 &\quad + 2 \widehat{x}^T (c \otimes PFC) \widehat{\Theta}.
 \end{aligned}$$

Recalling that $\Upsilon = \lambda(B^T P \bar{x}) + I_n \otimes u_0(t)$, ones obtain:

$$\begin{aligned}
 &-2 \widehat{x}^T (\bar{L} \otimes PB) \left(\theta \left(B^T P \bar{x} \right) + I_n \otimes u_0(t) \right) \\
 &\leq -2 \sum_{i=1}^N a_{i0} \widehat{x}_i^T PB \left(\theta_i \left(B^T P \widehat{x}_i \right) + u_0(t) \right) \\
 &\quad - 2 \sum_{i=1}^N |a_{i0}| \widehat{x}_i^T PB \times \left(\theta_i \left(B^T P \widehat{x}_i \right) - \theta_i \left(B^T P \widehat{x}_j \right) \right) \\
 &\leq 2(u_{\max} - 1) \sum_{i=1}^N a_{i0} \left| B^T P \widehat{x}_i \right| \\
 &\leq 0 \tag{35}
 \end{aligned}$$

Based on (9) and (19), one has:

$$\begin{aligned}
 &2 \widehat{x}^T (DL_1 \otimes P\Phi) \bar{W} \\
 &\leq 2 \widehat{x}^T (L_1 \otimes P) (D \otimes \Phi) \bar{W} \\
 &\leq 2 \sum_{i=1}^N a_i \left\| \widehat{x}_i^T P \right\| \cdot \|d_i(\omega(\widehat{x}_i) - d_i\omega(\widehat{x}_0))\| \\
 &\leq 2k \sum_{i=1}^N \left\| \widehat{x}_i^T P \right\| \cdot \|\widehat{x}_i\| \\
 &\leq \widehat{x}^T \left[I_N \otimes k^2 PP + I_n \right] \widehat{x}. \tag{36}
 \end{aligned}$$

Noting that $\Xi = (PA + A^T P - 2PBB^T P) < 0$, $\Theta = (QA - 2C^T C + A^T Q) < 0$, $K = -B^T P$, $F = -Q^{-1} C^T$, and $u_{\max} < 1$, ones obtain that:

$$\begin{aligned}
 \dot{V}_1 &\leq \widehat{x}^T (I_N \otimes \Xi) \widehat{x} - 2 \widehat{x}^T (c \otimes PBK) \widehat{\delta} \\
 &\quad + 2 \widehat{x}^T (c \otimes PFC) \widehat{\chi} + 2 \widehat{x}^T (DL_1 \otimes P\Phi) \bar{W} \\
 &\quad + \sum_{i=1}^N \widehat{\chi}^T (I_N \otimes \Theta) \widehat{\chi} \\
 &\leq \widehat{x}^T \left(I_N \otimes \Xi + k^2 PP + I_n \right) \widehat{x} \\
 &\quad - 2 \widehat{x}^T (c \otimes PBK) \widehat{\delta} + 2 \widehat{x}^T (c \otimes PFC) \widehat{\chi} \\
 &\quad + \sum_{i=1}^N \widehat{\chi}^T (I_N \otimes \Theta) \widehat{\chi} \tag{37}
 \end{aligned}$$

According to **Theorem 1** and Schur's Lemma (**Lemma 3**), it can be determined that $PA + A^T P - 2PBB^T P + k^2 PP + I_n$ is negative definite.

From Young's inequality, $2 \widehat{x}^T (c \otimes PFC) \widehat{\chi}$ and $\sum_{i=1}^N \widehat{x}^T (I_N \otimes \Theta) \widehat{\chi}$ in (37) can be transformed into:

$$\begin{aligned}
 &-2 \widehat{x}^T (c \otimes PBK) \widehat{\delta} \\
 &\leq \frac{4\lambda_{\max}^2(PBB^T P)}{\lambda_{\min}(\Xi)\lambda_{\min}(\Theta)} \widehat{\delta}^T [c \otimes \Theta] \widehat{\delta} - \frac{1}{4} \widehat{x}^T (c \otimes \Xi) \widehat{x}. \tag{38}
 \end{aligned}$$

$$\begin{aligned}
 &2 \widehat{x}^T (c \otimes PFC) \widehat{\chi} \\
 &\leq \frac{4\lambda_{\max}^2(PFCC^T F^T P)}{\lambda_{\min}(\Xi)\lambda_{\min}(\Theta)} \widehat{\chi}^T [c \otimes \Theta] \widehat{\chi} - \frac{1}{4} \widehat{x}^T (c \otimes \Xi) \widehat{x}. \tag{39}
 \end{aligned}$$

Substituting (36), (38), and (39) into (34), yields

$$\begin{aligned}
 \dot{V}_1 &\leq -\frac{1}{2} \widehat{x}^T \left(I_N \otimes \Xi + k^2 PP + I_n \right) \widehat{x} \\
 &\quad + \frac{4\lambda_{\max}^2(PBB^T P)}{\lambda_{\min}(\Xi)\lambda_{\min}(\Theta)} \widehat{\delta}^T [c \otimes \Theta] \widehat{\delta} \\
 &\quad + \left(1 + \frac{4\lambda_{\max}(PFCC^T F^T P)}{\lambda_{\min}(\Xi)\lambda_{\min}(\Theta)} \right) \widehat{\chi}^T [c \otimes \Theta] \widehat{\chi} \tag{40}
 \end{aligned}$$

let $\rho_1 = 4\lambda_{\max}^2(PBB^T P) / \lambda_{\min}(\Xi)\lambda_{\min}(\Theta)m$, $\rho_2 = 1 + 4\lambda_{\max}(PFCC^T F^T P) / \lambda_{\min}(\Xi)\lambda_{\min}(\Theta)$, we have:

$$\begin{aligned}
 \dot{V}_1 &\leq -\frac{1}{2} \widehat{x}^T \left(I_N \otimes \Xi + k^2 PP + I_n \right) \widehat{x} \\
 &\quad + \rho_2 \widehat{\chi}^T [c \otimes \Theta] \widehat{\chi} + \rho_1 \widehat{\delta}^T [c \otimes \Theta] \widehat{\delta}. \tag{41}
 \end{aligned}$$

According to (31) and (32), the derivative of V_2 is represented by:

$$\begin{aligned} \dot{V}_2 &= 2 \sum_{i=1}^N e_i^T Q \dot{e}_i + 2e_0^T Q \dot{e}_0 \\ &= e_i^T [I_N \otimes \Theta] e_i + e_0^T [I_N \otimes \Theta] e_0 e_i^T (I_N \otimes QBM) \tilde{\omega}_i \\ &\quad + e_0^T QBM \tilde{\omega}_0 + \tilde{\omega}_i^T (I_N \otimes M^T B^T Q) e_i \\ &\quad + \tilde{\omega}_0^T M^T B^T Q e_0 \\ &= \bar{e}^T [I_{N+1} \otimes \Theta] \bar{e} + \bar{e}^T (I_{N+1} \otimes QBM) \bar{\omega} \\ &\quad + \bar{\omega}^T (I_N \otimes M^T B^T Q) \bar{e}. \end{aligned} \quad (42)$$

where $\tilde{\omega}_i = \omega(\hat{x}_i) - \omega(x_i)$, $\tilde{\omega}_0 = \omega(\hat{x}_0) - \omega(x_0)$, $\bar{\omega}^T = [\tilde{\omega}_0^T, \tilde{\omega}_i^T]^T$, $\bar{e}^T = [e_0^T, e_i^T]^T$. By using the Lipschitz condition, it can be found that

$$\begin{aligned} &2\mu_1 (\omega(\hat{x}_i) - \omega(x_i))^T (\hat{x}_i - x_i) \\ &\leq 2k\mu_1 (\hat{x}_i - x_i)^T (\hat{x}_i - x_i) \\ &2\mu_2 [(\omega(\hat{x}_i) - \omega(x_i))^T (\omega(\hat{x}_i) - \omega(x_i))] \\ &\quad - 2\mu_2 [\rho (\hat{x}_i - x_i)^T (\hat{x}_i - x_i)] \\ &\leq 2\eta\mu_2 (\hat{x}_i - x_i)^T (\omega(\hat{x}_i) - \omega(x_i)) \end{aligned} \quad (43)$$

where μ_1, μ_2 . Subsequently, equation (43) can be rewritten as:

$$\begin{aligned} &2\mu_1 [\bar{\omega}^T \bar{e} - k\bar{e}^T \bar{e}] \leq 0, \\ &2\mu_2 [\bar{\omega}^T \bar{\omega} - \rho\bar{e}^T \bar{e} - \eta\bar{e}^T \bar{\omega}] \leq 0, \end{aligned} \quad (44)$$

Substituting (44) into (42), yields

$$\begin{aligned} \dot{V}_2 &\leq \bar{e}^T [I_{N+1} \otimes (\Theta + 2\mu_1 k I_N + 2\mu_2 \rho I_N)] \bar{e} \\ &\quad + \bar{e}^T (I_{N+1} \otimes QBM - \mu_1 I_N + \mu_2 \eta I_N) \bar{\omega} \\ &\quad + \bar{\omega}^T (I_N \otimes M^T B^T Q - \mu_1 I_N + \mu_2 \eta I_N) \bar{e} \\ &\quad - 2\mu_2 \bar{\omega}^T \bar{\omega}. \end{aligned} \quad (45)$$

Since $\Pi = \begin{bmatrix} \hat{x}^T & \hat{\delta}^T & \hat{\chi}^T & \hat{e}^T & \hat{\omega}^T \end{bmatrix}^T$, we have

$$\begin{aligned} V &= V_1 + V_2, \\ \dot{V} &\leq \Pi \begin{bmatrix} I_N \otimes \Delta_1 & 0 \\ 0 & I_N \otimes \Delta_2 \end{bmatrix} \Pi, \end{aligned} \quad (46)$$

where

$$\Delta_1 = \begin{bmatrix} -\frac{1}{2} (I_N \otimes \Xi + k^2 PP + I_n) & & \\ & \rho_1 [c \otimes \Theta] & \\ & & \rho_2 [c \otimes \Theta] \end{bmatrix}, \quad (47)$$

$$\Delta_2 = \begin{bmatrix} \Theta + 2\mu_1 k I_N + 2\mu_2 \rho I_N & QBM - \mu_1 I_N + \mu_2 \eta I_N \\ * & -2\mu_2 I_N \end{bmatrix}, \quad (48)$$

According to Schur's Lemma (Lemma 3), under conditions (10), (21), and (22), \dot{V} will be negative definite. According to (46) and Barbalat's Lemma (Lemma 5), one gets $\lim_{t \rightarrow \infty} \tilde{\varepsilon}(t) = 0$, which indicates that

$$\lim_{t \rightarrow \infty} \|x_i - f_i(t) - d_i x_0\| = 0 \quad (49)$$

Thus, the proof of BTVF for MAS is completed.

V. NUMERICAL RESULT

Assume the directed communication graph of MAS is given by Fig.1, which contains one leader (numbered 0) and eight followers (numbered 1 to 8). The model of the AUV is shown in Fig.2.

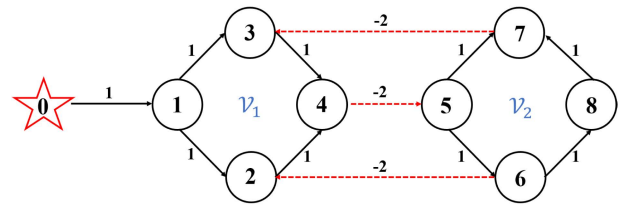


FIGURE 1. The communication topology of the constructed MAS (the black line indicates a cooperation relationship and the red line indicates a competition relationship).

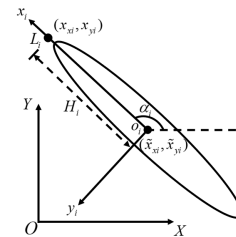


FIGURE 2. The i_{th} AUV.

Consider the formation of nine AUVs in waters of constant depth from the horizontal. Select a reference coordinate system XOY at the same altitude of the ocean, and the coordinate system of i_{th} AUV own is $x_i o_i y_i$. The o_i is located at the center of mass of each AUV. Select a point L_i outside the i_{th} AUV for subsequent formation control, the coordinates are expressed as $p_i = (x_{xi}, x_{yi})$. Set the position vector of i_{th} AUV as $\tilde{p}_i = [\tilde{x}_{xi}, \tilde{x}_{yi}, \alpha_i]$ and the velocity vector as $\gamma_i = [v_i, \omega_i]$. Since the AUV cannot move along the axis y_i under water, i.e., it cannot produce a lateral shift, the dimension of the velocity vector $\gamma_i \in \mathbb{R}^2$ is smaller than the position vector $\tilde{p}_i \in \mathbb{R}^3$, so Fig.2 is a non-complete mechanical system of the AUV. The relationship between $\tilde{x}_{xi}, \tilde{x}_{yi}, \alpha_i$, and ω can be obtained as:

$$\begin{bmatrix} \tilde{x}_{xi} \\ \tilde{x}_{yi} \end{bmatrix} = \begin{bmatrix} u_{ix} \\ u_{iy} \end{bmatrix} = \begin{bmatrix} v_i \cos \alpha_i \\ v_i \sin \alpha_i \end{bmatrix} \quad \dot{\alpha}_i = \omega \quad (50)$$

The coordinates of L_i are denoted as:

$$\begin{bmatrix} x_{xi} \\ x_{yi} \end{bmatrix} = \begin{bmatrix} \tilde{x}_{xi} \\ \tilde{x}_{yi} \end{bmatrix} + H_i \begin{bmatrix} \cos \alpha_i \\ \sin \alpha_i \end{bmatrix} \quad (51)$$

where H_i is a constant and represents the distance from o_i to L_i . Take $H_i = 1$. From (50) and (51) we obtain:

$$\gamma_i = R(\alpha_i)\dot{p}_i \quad (52)$$

where

$$R(\alpha_i) = \begin{bmatrix} \cos \alpha_i & \sin \alpha_i \\ -(\sin \alpha_i)/H_i & (\cos \alpha_i)/H_i \end{bmatrix}, \quad H_i \neq 0 \quad (53)$$

The significance of this simplification is that we can control the AUV directly by controlling the point L_i . The validity of the designed output feedback-based control strategy is verified by a system consisting of nine AUVs. The AUV model after simplification is represented by (4) and (5), referring to [25] and [47], we can set the parameter matrix as

$$A = \begin{bmatrix} 0 & 1 & 0 & 0 \\ 0 & 0 & 0 & 0 \\ 0 & 0 & 0 & 1 \\ 0 & 0 & 0 & 0 \end{bmatrix}, \quad B = \begin{bmatrix} 0 & 0 \\ 1 & 0 \\ 0 & 0 \\ 0 & 1 \end{bmatrix}, \quad x_i = \begin{bmatrix} x_{xi} \\ v_{xi} \\ x_{yi} \\ v_{yi} \end{bmatrix},$$

$$C = \begin{bmatrix} 1 & 1 & 0 & 0 \\ 0 & 0 & 1 & 1 \end{bmatrix}, \quad v_i = \begin{bmatrix} v_{xi} \\ v_{yi} \end{bmatrix}, \quad u_i = \begin{bmatrix} u_{ix} \\ u_{iy} \end{bmatrix}$$

In **Fig.1**, all AUVs are divided into two groups, the black line represents the cooperative relationship between two agents in the same group, and the red line means the competitive relationship between agents in different groups. Meanwhile, the followers are split into two sets: $V_a = \{1, 2, 3, 4\}$, $V_b = \{5, 6, 7, 8\}$. For the cooperation network illustrated in **Fig.1**, the value of d_i represents the cooperative and competitive relationship between each follower and leader. It can be expressed as $D = \{1, 1, 1, 1, -1, -1, -1, -1\}$. $\Phi = BM = B \begin{bmatrix} 1 & 0 \\ 0 & 1 \end{bmatrix}$. Furthermore, calculations show that $k = 1$ satisfies the Lipschitz condition, i.e. **Assumption 4** for the nonlinear MAS. For the protocol of output feedback, $u_{max} = 0.1$ is selected. It indicated that $\|u_o(t)\| < 0.1$, so the leader's control input be expressed as:

$$u_0 = \begin{cases} \begin{bmatrix} 0.05, & 0.07 \end{bmatrix}^T, & t \leq 25 \text{ s} \\ \begin{bmatrix} 0, & -0.07 \end{bmatrix}^T, & 25 \text{ s} < t \leq 40 \text{ s} \\ \begin{bmatrix} 0, & -0.03 \end{bmatrix}^T, & 40 \text{ s} < t \leq 60 \text{ s} \\ \begin{bmatrix} 0, & 0 \end{bmatrix}^T, & t \leq 100 \text{ s} \end{cases}$$

The control inputs of the leader are plotted along with time in **Fig.3**. The formation control vector $f_i(t)$ and the formation compensational vector $v_i(t)$ of BTVF for follower i can be expressed as:

$$f_i(t) = \begin{bmatrix} \rho_1 \sin(\tau_1 t + 2\pi\lambda(i)/n_1) \\ \rho_1 \tau_1 \cos(\tau_1 t + 2\pi\lambda(i)/n_1) \\ \rho_1 \cos(\tau_1 t + 2\pi\lambda(i)/n_1) \\ -\rho_1 \tau_1 \sin(\tau_1 t + 2\pi\lambda(i)/n_1) \end{bmatrix}, \quad i \in V_a,$$

$$f_i(t) = \begin{bmatrix} \rho_2 \sin(\tau_2 t + 2\pi\lambda(i)/n_2) \\ \rho_2 \tau_2 \cos(\tau_2 t + 2\pi\lambda(i)/n_2) \\ \rho_2 \cos(\tau_2 t + 2\pi\lambda(i)/n_2) \\ -\rho_2 \tau_2 \sin(\tau_2 t + 2\pi\lambda(i)/n_2) \end{bmatrix}, \quad i \in V_b,$$

$$v_i(t) = \begin{bmatrix} -\rho_1 \tau_1^2 \sin(\tau_1 t + 2\pi\lambda(i)/n_1) \\ -\rho_1 \tau_1^2 \cos(\tau_1 t + 2\pi\lambda(i)/n_1) \end{bmatrix}, \quad i \in V_a,$$

$$v_i(t) = \begin{bmatrix} -\rho_2 \tau_2^2 \sin(\tau_2 t + 2\pi\lambda(i)/n_2) \\ -\rho_2 \tau_2^2 \cos(\tau_2 t + 2\pi\lambda(i)/n_2) \end{bmatrix}, \quad i \in V_b,$$

where $\lambda(i) = i - 1$.

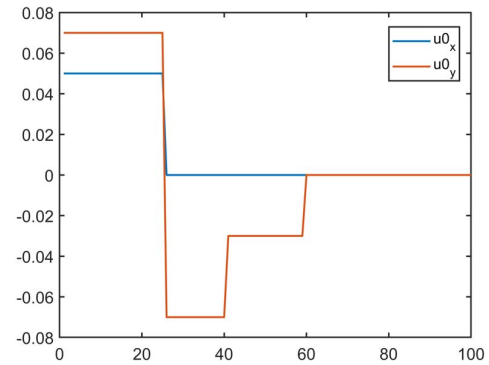


FIGURE 3. The trajectories curves of u .

TABLE 1. Setting of system parameters.

Constants	Value	Explanation
$\rho_1 = \rho_2$	8	Radius of formation
$\tau_1 = \tau_2$	0.25	Angular velocity
$n_1 = n_2$	4	The number of followers in each team
μ_1	1	The parameters of the one-sided Lipschitz condition and inequality (24),(47), and(48)
μ_2	0.05	
k	1	
η_1	-10	
η_2	-9	

The system satisfies the one-sided Lipschitz condition when the constant $k = 1$ in **Assumption 4** or there exists a region $M = \{x_i \in \mathbb{R}^2, \|x_i\| \leq \bar{m}\}$. The \bar{m} can be expressed as $\bar{m} = \min\left(\sqrt[4]{\eta_2 + \frac{\eta_1^2}{4}}, \sqrt{-\frac{\eta_1}{4}}\right)$. Due to the bipartite formation characteristics, the nature of the one-sided Lipschitz condition and (24), (47), (48), we can select scalars as shown in Table 1. Where n_1 and n_2 represents the number of followers in V_a and V_b , respectively.

The solution to inequality (23) is obtained by using the LMI toolbox of MATLAB:

$$P = I_2 \otimes \begin{bmatrix} 2.0051 & -0.6684 \\ -0.6684 & 0.6684 \end{bmatrix},$$

$$Q = I_2 \otimes \begin{bmatrix} 1.5715 & -0.0352 \\ -0.0352 & 1.4763 \end{bmatrix},$$

The gain matrix is given as:

$$K = I_2 \otimes \begin{bmatrix} -0.7481 & -2.2443 \end{bmatrix},$$

$$F = I_2 \otimes \begin{bmatrix} -0.6518 \\ -0.6929 \end{bmatrix}.$$

The Fig.4 illustrates the final formation achieved by bipartite formation control algorithm and the path curve of the leader and followers over time in the absence of external disturbances. At that time the system equations in (4) and (5) without $\Phi\omega(x_i)$, ($i = 0, \dots, N$). The asterisk “*” represents the position of the eight followers in formation, and a red pentagram represents the position of the leader. In V_a , four followers surround the leader and move forward to keep a specific angle and distance from the leader. In V_b , four followers move forward to keep a specific angle and distance from the virtual leader. The leader and virtual leader have opposite states. It is clear from Fig.5 that the agents in different teams finally evolve into two opposite states. The agents in V_a converge to x , while those in V_b converge to the opposite $-x$. Fig.6 illustrates the observation error between x_i and \hat{x}_i , which indicates that e_i and e_0 converge to zero asymptotically.

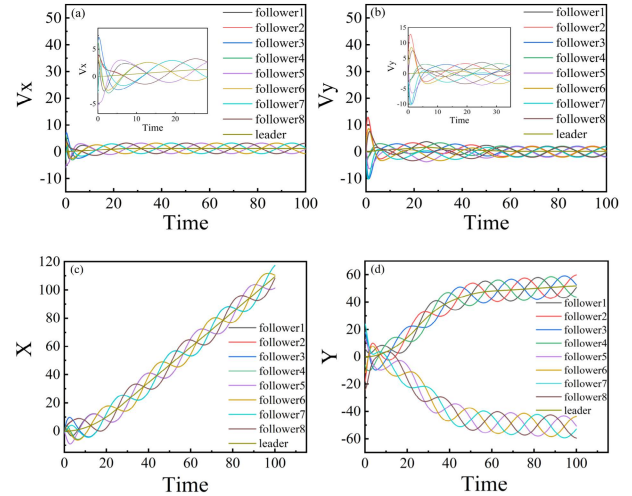


FIGURE 5. (a), (b) The velocity variation of of all agents. (c), (d) The position of all agents.

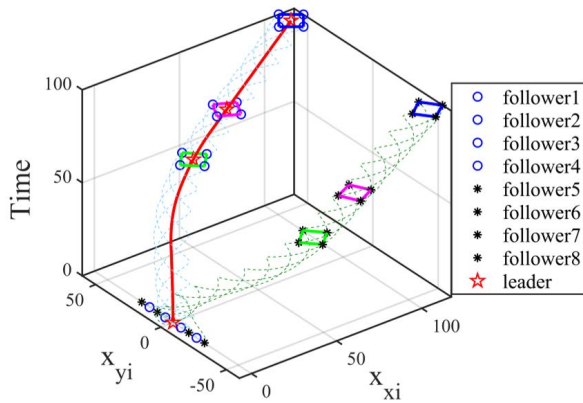


FIGURE 4. The snapshots of the multi-agent formation.

Next, the influence of external disturbance on the bipartite formation of the MAS is considered. The external disturbance for each agent is assumed as:

$$\omega_0 = [0.5 \cos(6t); 0.4 \sin(8t)]^T,$$

$$\omega_1 = [0.5 \cos(3t); 0.8 \sin(4t)]^T,$$

$$\omega_2 = [0.4 \cos(2t); 0.3 \sin(5t)]^T,$$

$$\omega_3 = [0.3 \cos(4t); 0.5 \sin(3t)]^T,$$

$$\omega_4 = [0.4 \cos(6t); 0.6 \sin(7t)]^T,$$

$$\omega_5 = [0.5 \cos(7t); 0.3 \sin(7t)]^T,$$

$$\omega_6 = [0.6 \cos(7t); 0.3 \sin(7t)]^T,$$

$$\omega_7 = [0.4 \cos(6t); 0.6 \sin(7t)]^T,$$

$$\omega_8 = [0.4 \cos(6t); 0.5 \sin(7t)]^T.$$

The Fig.7 illustrates the final formation achieved by bipartite formation control algorithm and the path curve of the leader and followers over time in the presence of external

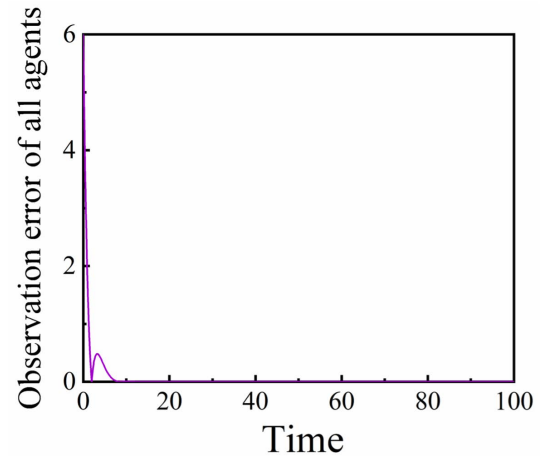


FIGURE 6. The observation error between and of the system without nonlinear term.

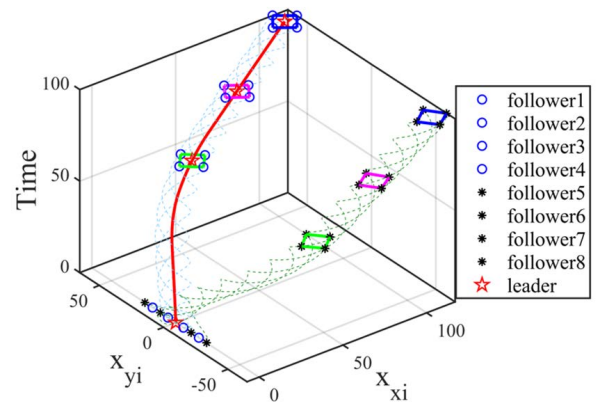


FIGURE 7. The snapshots of the multi-agent formation under nonlinear disturbance.

disturbance. It indicates that the MAS can ultimately reach the desired formation under disturbances. Fig.8 presents the velocity variation of all the agents under disturbance. It can

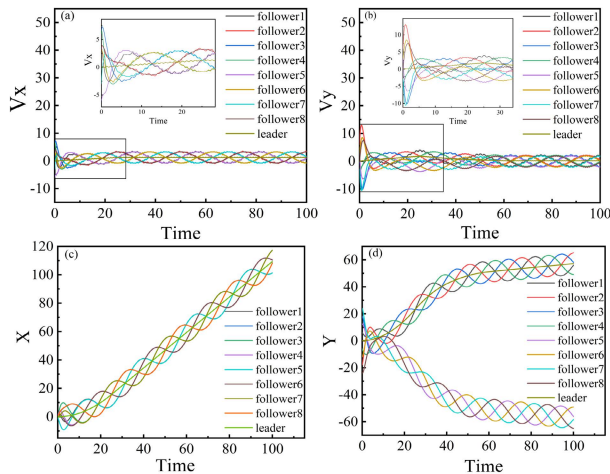


FIGURE 8. (a), (b) The velocity variation of all agents under nonlinear disturbance. (c), (d) The position of all agents under nonlinear disturbance.

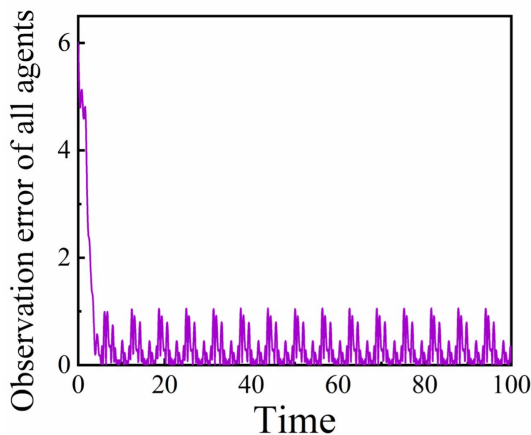


FIGURE 9. The observation error between and under nonlinear disturbance.

be seen that the agents in the two sets V_a and V_b converge to two opposite states. The curve of the observation error between x_i and \hat{x}_i for the MAS under nonlinear disturbance is plotted in Fig.9. It is obvious that external nonlinear disturbances have a certain influence on the error of the system, but their fluctuations are stable within a certain range. This phenomenon verifies the validity of the above-mentioned theory for adaptive bipartite tracking formation of MASs under external disturbances. The comparison of Fig.5 and Fig.8 indicates that external disturbances affect the speed and trajectory of the AUV at a given moment, but no influence on the formation of the AUV at that moment, which further demonstrates the suppression of external disturbances by the adaptive control strategy based on output feedback.

VI. CONCLUSION

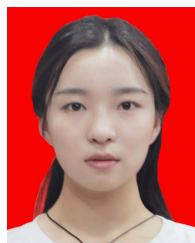
This paper investigates the network model with cooperation-competition relationships. First, positive and negative edges are adopted represent the cooperative behavior and

competition behavior between agents, respectively. Then an adaptive control protocol is proposed for nonlinear MAS for the leader-follower BTVF, and the corresponding algorithm proofs are given. The main advantage of this solution is that the global state of all agents does not need to be known. Next, the Lipschitz property is exploited to solve the nonlinear terms in this system. Subsequently, the stability of system is analyzed and verified by the Lyapunov candidate function associated with the error function. Finally, we analyze the AUV fixed-depth motion model, simplify this model to a mass point model, construct a MAS containing nine AUVs, and validate the effectiveness of the proposed strategy. The analysis of the numerical simulation results show that the MASs can achieve the expected formation with external disturbance. The further work will focus on the application of this algorithm to multi-AUV cooperative control for complex ocean environment observations.

REFERENCES

- [1] Q. Deng, J. Wu, T. Han, Q.-S. Yang, and X.-S. Cai, "Fixed-time bipartite consensus of multi-agent systems with disturbances," *Phys. A, Stat. Mech. Appl.*, vol. 516, pp. 37–49, Feb. 2019.
- [2] T. Han, Z.-H. Guan, B. Xiao, J. Wu, and X. Chen, "Distributed output consensus of heterogeneous multi-agent systems via an output regulation approach," *Neurocomputing*, vol. 360, pp. 131–137, Sep. 2019.
- [3] S. Li, J. Zhang, X. Li, F. Wang, X. Luo, and X. Guan, "Formation control of heterogeneous discrete-time nonlinear multi-agent systems with uncertainties," *IEEE Trans. Ind. Electron.*, vol. 64, no. 6, pp. 4730–4740, Feb. 2017.
- [4] N. E. Leonard, D. A. Paley, R. E. Davis, D. M. Fratantoni, F. Lekien, and F. M. Zhang, "Coordinated control of an underwater glider fleet in an adaptive ocean sampling field experiment in Monterey Bay," *J. Field Robot.*, vol. 27, no. 6, pp. 718–740, Sep. 2010.
- [5] H. R. Karimi, H. Zhang, and S. Ding, "Advanced methods in control and signal processing for complex marine systems," *ISA Trans.*, vol. 78, pp. 1–2, Jul. 2018.
- [6] H. B. Du, Z. Q. Chen, and G. H. Wen, "Leader-following attitude consensus for spacecraft formation with rigid and flexible spacecraft," *J. Guid. Control Dyn.*, vol. 39, no. 4, pp. 941–948, 2016.
- [7] B. Zhu, A. H. B. Zaini, and L. Xie, "Distributed guidance for interception by using multiple rotary-wing unmanned aerial vehicles," *IEEE Trans. Ind. Electron.*, vol. 64, no. 7, pp. 5648–5656, Mar. 2017.
- [8] Z. Li and J. Chen, "Robust consensus of linear feedback protocols over uncertain network graphs," *IEEE Trans. Autom. Control*, vol. 62, no. 8, pp. 4251–4258, Mar. 2017.
- [9] Q. Ma, S. Y. Xu, F. L. Lewis, B. Y. Zhang, and Y. Zou, "Cooperative output regulation of singular heterogeneous multiagent systems," *IEEE Trans. Cybern.*, vol. 46, no. 6, pp. 1471–1475, Jun. 2016.
- [10] J. Mei, W. Ren, and J. Chen, "Distributed consensus of second-order multi-agent systems with heterogeneous unknown inertias and control gains under a directed graph," *IEEE Trans. Autom. Control*, vol. 61, no. 8, pp. 2019–2034, Aug. 2016.
- [11] W. Ren and R. W. Beard, "Consensus seeking in multiagent systems under dynamically changing interaction topologies," *IEEE Trans. Autom. Control*, vol. 50, no. 5, pp. 655–661, May 2005.
- [12] R. Olfati-Saber and R. M. Murray, "Consensus problems in networks of agents with switching topology and time-delays," *IEEE Trans. Autom. Control*, vol. 49, no. 9, pp. 1520–1533, Sep. 2004.
- [13] W. Yu, G. Chen, and M. Cao, "Some necessary and sufficient conditions for second-order consensus in multi-agent dynamical systems," *Automatica*, vol. 46, no. 6, pp. 1089–1095, Jun. 2010.
- [14] X. Feng, Y. Yang, and D. Wei, "Adaptive fully distributed consensus for a class of heterogeneous nonlinear multi-agent systems," *Neurocomputing*, vol. 428, pp. 12–18, Mar. 2021.
- [15] T. Vicsek, A. Czirók, E. Ben-Jacob, I. Cohen, and O. Shochet, "Novel type of phase transition in a system of self-driven particles," *Phys. Rev. Lett.*, vol. 75, no. 6, pp. 1226–1229, 1995.

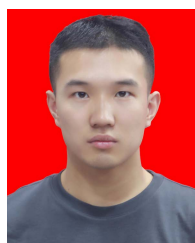
- [16] A. Jadbabaie, J. Lin, and A. S. Morse, "Coordination of groups of mobile autonomous agents using nearest neighbor rules," *IEEE Trans. Autom. Control*, vol. 48, no. 6, pp. 988–1001, Jun. 2003.
- [17] X. Dong, Y. Zhou, Z. Ren, and Y. Zhong, "Time-varying formation control for unmanned aerial vehicles with switching interaction topologies," *Control Eng. Pract.*, vol. 46, pp. 26–36, Jan. 2016.
- [18] J. Guo, G. Yan, and Z. Lin, "Local control strategy for moving-target-enclosing under dynamically changing network topology," *Syst. Control Lett.*, vol. 59, no. 10, pp. 654–661, Oct. 2010.
- [19] D. Ye, M.-M. Chen, and H.-J. Yang, "Distributed adaptive event-triggered fault-tolerant consensus of multiagent systems with general linear dynamics," *IEEE Trans. Cybern.*, vol. 49, no. 3, pp. 757–767, Mar. 2017.
- [20] F. Baghbani, M.-R. Akbarzadeh-T, and M.-B. N. Sistani, "Cooperative adaptive emotional neuro-control for a class of higher-ordered heterogeneous uncertain nonlinear multi-agent systems," *Neurocomputing*, vol. 447, pp. 196–212, Mar. 2021.
- [21] G. Wang, C. Wang, L. Li, and Z. Zhang, "Designing distributed consensus protocols for second-order nonlinear multi-agents with unknown control directions under directed graphs," *J. Franklin Inst.*, vol. 354, pp. 571–592, Jan. 2017.
- [22] G. Wang, C. Wang, and L. Li, "Fully distributed low-complexity control for nonlinear strict-feedback multiagent systems with unknown dead-zone inputs," *IEEE Trans. Syst., Man, Cybern., Syst.*, vol. 50, no. 2, pp. 421–431, Feb. 2020.
- [23] G. Wang, C. Wang, and Y. Shen, "Distributed adaptive leader-following tracking control of networked Lagrangian systems with unknown control directions under undirected/directed graphs," *Int. J. Control*, vol. 92, no. 12, pp. 2886–2898, Dec. 2019.
- [24] C. Altafini, "Consensus problems on networks with antagonistic interactions," *IEEE Trans. Autom. Control*, vol. 58, no. 4, pp. 935–946, Oct. 2013.
- [25] G. Wen, H. Wang, X. Yu, and W. Yu, "Bipartite tracking consensus of linear multi-agent systems with a dynamic leader," *IEEE Trans. Circuits Syst. II, Exp. Briefs*, vol. 65, no. 9, pp. 1204–1208, Sep. 2018.
- [26] C. Yan, W. Zhang, X. Li, and H. Su, "Adaptive bipartite time-varying formation control for multi-agent systems on directed graph," in *Proc. 39th Chin. Control Conf. (CCC)*, Jul. 2020, pp. 4701–4706.
- [27] R. Cui, S. S. Ge, B. V. E. How, and Y. S. Choo, "Leader-follower formation control of underactuated autonomous underwater vehicles," *Ocean Eng.*, vol. 37, nos. 17–18, pp. 1491–1502, Dec. 2010.
- [28] Y.-Y. Chen, Y. Zhang, and Z.-Z. Wang, "An adaptive backstepping design for formation tracking motion in an unknown Eulerian specification flow-field," *J. Franklin Inst.*, vol. 354, no. 14, pp. 6217–6233, Sep. 2017.
- [29] D. Meng, Y. Jia, J. Du, and J. Zhang, "On iterative learning algorithms for the formation control of nonlinear multi-agent systems," *Automatica*, vol. 50, no. 1, pp. 291–295, 2014.
- [30] W. Wang, C. Huang, C. Huang, J. Cao, J. Lu, and L. Wang, "Bipartite formation problem of second-order nonlinear multi-agent systems with hybrid impulses," *Appl. Math. Comput.*, vol. 370, Apr. 2020, Art. no. 124926.
- [31] M. Shahvali, M.-B. Naghibi-Sistani, and J. Askari, "Adaptive output-feedback bipartite consensus for nonstrict-feedback nonlinear multi-agent systems: A finite-time approach," *Neurocomputing*, vol. 318, pp. 7–17, Nov. 2018.
- [32] W. Guo and W. Luo, "Pinning adaptive-impulsive consensus of the multi-agent systems with uncertain perturbation," *Neurocomputing*, vol. 275, pp. 2329–2340, Jan. 2018.
- [33] X. Yang and J. Cao, "Hybrid adaptive and impulsive synchronization of uncertain complex networks with delays and general uncertain perturbations," *Appl. Math. Comput.*, vol. 227, pp. 480–493, Jan. 2014.
- [34] L. Zhao, J. Yu, and C. Lin, "Command filter based adaptive fuzzy bipartite output consensus tracking of nonlinear cooperation multi-agent systems with input saturation," *ISA Trans.*, vol. 80, pp. 187–194, Sep. 2018.
- [35] X. Nan, Y. Lv, and Z. Duan, "Bipartite consensus tracking for antagonistic topologies with leader's unknown input," *Asian J. Control*, vol. 24, no. 2, pp. 547–561, Mar. 2022.
- [36] H. Zhao, L. Peng, and H. Yu, "Quantized model-free adaptive iterative learning bipartite consensus tracking for unknown nonlinear multi-agent systems," *Appl. Math. Comput.*, vol. 412, Jan. 2022, Art. no. 126582.
- [37] J. Qin, W. Fu, W. X. Zheng, and H. Gao, "On the bipartite consensus for generic linear multiagent systems with input saturation," *IEEE Trans. Cybern.*, vol. 47, no. 8, pp. 1948–1958, Aug. 2017.
- [38] E. E. Yaz, "Linear matrix inequalities in system and control theory," *Proc. IEEE*, vol. 86, no. 12, pp. 2473–2474, Dec. 1998.
- [39] Y. Kang, D.-H. Zhai, G.-P. Liu, Y.-B. Zhao, and P. Zhao, "Stability analysis of a class of hybrid stochastic retarded systems under asynchronous switching," *IEEE Trans. Autom. Control*, vol. 59, no. 6, pp. 1511–1523, Jun. 2014.
- [40] Y. J. Liu, S. C. Tong, D. Wang, T. S. Li, and C. L. P. Chen, "Adaptive neural output feedback controller design with reduced-order observer for a class of uncertain nonlinear SISO systems," *IEEE Trans. Neural Netw.*, vol. 22, no. 8, pp. 1328–1334, Aug. 2011.
- [41] Y.-J. Liu, C. L. P. Chen, G.-X. Wen, and S. Tong, "Adaptive neural output feedback tracking control for a class of uncertain discrete-time nonlinear systems," *IEEE Trans. Neural Netw.*, vol. 22, no. 7, pp. 1162–1167, Jul. 2011.
- [42] Z. Peng, L. Liu, and J. Wang, "Output-feedback flocking control of multiple autonomous surface vehicles based on data-driven adaptive extended state observers," *IEEE Trans. Cybern.*, vol. 51, no. 9, pp. 4611–4622, Sep. 2021.
- [43] J. Yue, L. Liu, Z. Peng, D. Wang, and T. Li, "Data-driven adaptive extended state observer design for autonomous surface vehicles with unknown input gains based on concurrent learning," *Neurocomputing*, vol. 467, pp. 337–347, Jan. 2022.
- [44] C. Yan, W. Zhang, H. Su, and X. Li, "Adaptive bipartite time-varying output formation control for multiagent systems on signed directed graphs," *IEEE Trans. Cybern.*, early access, Mar. 11, 2021, doi: 10.1109/TCYB.2021.3054648.
- [45] H. Zhang, Z. Li, Z. Qu, and F. L. Lewis, "On constructing Lyapunov functions for multi-agent systems," *Automatica*, vol. 58, pp. 39–42, Aug. 2015.
- [46] J. Slotine and W. Li, *Applied Nonlinear Control*. Beijing, China: China Machine Press, 1991.
- [47] W. Jie, D. Qun, H. Tao, Y. Qing-Sheng, and Z. Heng, "Bipartite tracking consensus for multi-agent systems with Lipschitz-type nonlinear dynamics," *Phys. A, Stat. Mech. Appl.*, vol. 525, pp. 1360–1369, Jul. 2019.



LU LIU received the B.S. degree in measurement and control technology and instrumentation from the Taiyuan Institute of Technology, Taiyuan, China, in 2020. She is currently pursuing the M.S. degree with the State Key Laboratory of Dynamic Measurement Technology, School of Instrument and Electronics, North University of China, Taiyuan. Her current research interest includes the formation control of multi-agent systems.



DAN LIU received the Ph.D. degree in electronic science and technology from Xi'an Jiaotong University, Xi'an, China, in 2019. He is currently an Associate Professor with the School of Electrical and Control Engineering, North University of China, Taiyuan, China. His current research interests include underwater unmanned systems and multi-agent coordination control.



YUHANG MA received the B.S. degree in communication engineering from the North University of China, Taiyuan, China, in 2020, where he is currently pursuing the M.S. degree with the State Key Laboratory of Dynamic Measurement Technology, School of Instrument and Electronics. His current research interests include electronic information and communication.



CHENYU YANG received the B.S. degree in electrical engineering and automation from the Jiangxi University of Science and Technology, Taiyuan, China, in 2020. She is currently pursuing the M.S. degree with the State Key Laboratory of Dynamic Measurement Technology, School of Instrument and Electronics, North University of China, Taiyuan. Her current research interests include underwater submersible modeling and simulation.



ZENGXING ZHANG received the Ph.D. degree in applied micro-and nanosystems from the University of South-Eastern Norway, Norway, in 2022. He is currently a Lecturer with the School of Instrument and Electronics, North University of China, Taiyuan, China. His current research interest includes mico/nano sensors.



HUIYU ZHANG received the B.S. degree in electronic information engineering from Shanxi University, Taiyuan, China, in 2020. He is currently pursuing the M.S. degree with the State Key Laboratory of Dynamic Measurement Technology, School of Instrument and Electronics, North University of China, Taiyuan. His research interests include underwater cooperative strategy and submarine control algorithms.



ZHIDONG ZHANG received the Ph.D. degree in electromagnetic field and microwave technology from Southwest Jiaotong University, Chengdu, China, in 2009. He is currently an Associate Professor with the School of Instrument and Electronics, North University of China, Taiyuan, China. His current research interest includes mico/nano sensors.



BIN YAO received the B.A. degree in communication engineering from the North University of China, Taiyuan, China, in 2021, where he is currently pursuing the M.S. degree with the State Key Laboratory of Dynamic Measurement Technology, School of Instrument and Electronics. His research interests include embedded systems, a fusion of sensor information, and autonomous control algorithms for the unmanned underwater vehicle.



CHENYANG XUE received the Ph.D. degree in semiconductor materials from the National University of Science and Technology, Athens, Greece, in 2003. He is currently a Professor with the School of Instrument and Electronics, North University of China, Taiyuan, China. His research interests include novel micro/nano devices, solid spectroscopy, and micro-optical sensors.

...